ISSN (Online) 2456 -1304

International Journal of Science, Engineering and Management (IJSEM)

Volume 10 Issue 12 December 2023

Load Variation Response of a SOFC-TCC System with Green Hydrogen Generation by PEMEC in Core Substation with Renewable Penetration

[1] Shafirah Khairina Budiawan, [2] Shin'ya Obara

[1] [2] Kitami Institute of Technology, Japan
Corresponding Author Email: [1] m3225180014@std.kitami-it.ac.jp, [2] obara@mail.kitami-it.ac.jp

Abstract*— A SOFC triple combined cycle power generation, consisting of a solid oxide fuel cell and gas turbine combined cycle is revealed to give efficiency improvement while reducing the amount of emissions in power generation. It comes from the fact that the exhaust heat generated from a cycle is further utilized for power generation in the next cycle. Studies concerning its designs and optimizations have been previously investigated, including the characteristics of the system. This study provides a model of a SOFC-TCC system aimed to provide a robust and appropriate load response while maintaining frequency deviation under normal conditions. The green hydrogen generated by PEMEC in the study is powered by the surplus renewable power where after generation, it is then stored in a hydrogen tank. The SOFC-TCC system in the study managed to provide power in response to power demand accurately without any substantial delay. Also, the observed frequency deviation throughout the whole cycle is under the tolerable amount.

Keywords: frequency deviation, hydrogen generation, load response control, sofc-tcc modeling.

I. INTRODUCTION

The global temperature experienced a rapid increase in the past decades, which was marked by the start of the Industrial Revolution. This temperature increase is caused by the greenhouse gases trapped in the ozone. To keep the global temperature at a safe level, nations are required to achieve net zero emissions by 2050. As the power generation sector is the top contributor to those greenhouse gases, an immediate transition from conventional power generation to a more greener and sustainable power generation method is crucial.

Several of the currently available options are renewable sources, batteries, fuel cells and/or electrolyzers, and green fuels such as hydrogen and biofuel. One of the most preferred methods is renewable power generation. Due to its abundance in nature and its zero emissions, developments, and constructions have been massively promoted. Therefore, it can be assumed that a massive amount of renewable power penetration into the power grid will happen in the future.

However, one issue is that renewable sources, especially sun and wind are intermittent and therefore resulting in a fluctuative renewable power where the generated power is usually inadequate or surplus. This will directly affect the power system stability as there will be a difference in power demand and power generated. One of the most preferred strategies is by implementation of energy storage systems (ESS), mainly batteries. However, for long-term storage, batteries are not the most ideal option, rather, a fuel cell is preferred.

Previously, a study where an SOFC is coupled with a gas steam turbine combined cycle and a renewable power generation penetration was investigated. The study offers a method for countering renewable power fluctuation in the system by power generation by the SOFC-TCC [1].

SOFC and combined cycle power generation coupling was first mentioned by S. Veyo in 1996 the idea comes from the ability of SOFC to provide additional heat to the gas turbine operation where the efficiency is expected at approximately 85% [2]. In 2011, following suit, Mitsubishi developed a hydrogen-fueled high-temperature tubular SOFC-TCC system with an efficiency of 55% with a final target of 70% efficiency [3].

Following the study, a SOFC-TCC system modeling for load response management was performed. The study adopted the SOFC-TCC system and included a hydrogen generation and storage system. Rather, the load following response was inadequate and the observed frequency deviation surpasses the allowed threshold.

In a future scenario where a massive integration of renewable power in the system happens, this study proposes a triple combined cycle system of SOFC and combined cycle (SOFC-TCC) for the system's stabilization. As the combined cycle power plants possess inertia, the tendency of rotary machines, and turbines, to keep on rotating, this tendency is especially helpful as a first defense in case of small fluctuations. Thus, eliminating the need for a battery storage system. Furthermore, to align with the goal of sustainable energy and power generation, the system is equipped with an electrolyzer of proton exchange membrane electrolyzer (PEMEC) for green hydrogen generation and a hydrogen tank for storage.

This study will investigate the power generation performance of the SOFC-TCC system while maintaining the system stability observed through the resulting frequency deviation.

IFERP
connecting engineers... developing research

ISSN (Online) 2456 -1304

International Journal of Science, Engineering and Management (IJSEM)

Volume 10 Issue 12 December 2023

II. PROPOSED SYSTEM CONFIGURATION

The SOFC triple combined cycle is made up of a single SOFC unit and a gas steam turbine combined cycle unit. As the available renewable power is inconsistent and fluctuates, the SOFC-TCC is set to provide for the remaining power demand unfulfilled by renewable power. In the SOFC-TCC system, SOFC is the topping cycle and operates in high pressure and high temperature. The SOFC will provide for the power demand according to its equipment capacity, and the remaining will be supplied by the combined cycle.

The SOFC and combined cycle are interconnected by the generated heat at the SOFC outlet, which possesses a high potential for work, and is further utilized. The gas turbine combined cycle exploits this energy for further power generation. This results in less wasted energy and increased efficiency.

III. EQUIPMENT MODELING

A. Modeling of the SOFC

Solid Oxide Fuel Cell is a high-temperature fuel cell and typically operates between 600-1000°C and temperature directly affects the fuel cell's efficiency. Along the anode and cathode walls, two types of electrochemical reaction occurs, hydrogen oxidation and oxygen reduction. Air enters the cathode side, comes into contact with electrons, and forms oxygen ions. On the anode side, the fuel enters and reacts with oxygen ions producing water, heat, and electrons.

Modeling a SOFC is a complex process and for the sake of simplicity, a simplified design, which has been proven to be sufficient as the representation of SOFC operation, is used in this study. This study implements a previously analyzed SOFC model that uses methane fuel [1].

Table 1. Electrochemical Reaction in Sofc

Side	Reaction Name	Reaction	Reaction Rate
Anode	Hydrogen Oxidation	$H_2+O_2^-$→ H_2O+2e^-	r_{an}
Cathode	Oxygen Reduction	$0.5O_2+2e^-$ →O^{2-}	r_{ca}

As the fuel cell analyzed runs only on hydrogen fuel, the methane reforming reaction occurring in the previous study is neglected and the occurring reaction will only be hydrogen oxidation, at the anode side, and oxygen reduction, at the cathode side. The reaction rate for both reactions is directly related to the current value (I) where the F is the Faraday constant.

$$r_{an} = r_{ca} = \frac{I}{2F} \quad (1)$$

The transfer function of the SOFC system power output is based on [1]. The output of SOFC ($P_{SOFC,out}$) can be obtained by calculating the number of hydrogen moles inside the fuel cell (m_{H2in}) divided by the time constant of SOFC output (T_{SOFCs}).

$$P_{SOFC,out} = \frac{m_{H_2in}}{1 + T_{SOFC}s} \quad (2)$$

The fuel cell produces electricity and heat. A certain percentage of the produced heat is recovered and utilized for gas steam turbine combined cycle operation. The maximum heat recovery efficiency ($e_{H,MAX}$) is calculated by the following equation [4]. Where e_R represents fuel cell efficiency.

$$\varepsilon_{H.MAX} = 1 - \varepsilon_R \quad (3)$$

The amount of heat generated by a fuel cell (d_{HMAX}) is as seen in equation (4) and P_{fc} represents the electrical output of the fuel cell

$$d\dot{H}_{MAX} = \frac{(1-\varepsilon_R)P_{fc}}{\varepsilon_R} \quad (4)$$

B. Combined Cycle Power Plant Modeling

The topping cycle of the combined cycle is a gas turbine and the bottoming cycle is a steam turbine. The modeling of the whole system was based on [1] and [5].

1) Gas Turbine Compressor

The temperature of the compressor outlet (T_{ACout}) can be calculated by using the temperature of the compressor inlet (T_{ACin}). η_c, P_{ro}, W, and γ on the other hand are the compressor efficiency, compressor pressure ratio, air flow rate per unit (pu), and ratio of the specific heat.

$$T_{AC_{out}} = T_{AC_{in}}\left(1 + \frac{x-1}{\eta_c}\right) \quad (5)$$

2) Gas Turbine

The temperature of the gas turbine inlet (T_{Gin}) is equal to the sum of the compressor outlet temperature and the difference in rating between gas turbine inlet temperature ($T_{Gin,rat}$) and compressor outlet temperature ($T_{ACout,rat}$) times by the fuel flow rate (W_f).

$$T_{G_{in}} = T_{AC_{out}} + (T_{G_{in,rat}} - T_{AC_{out,rat}})W_f \quad (6)$$

On the other hand, the gas turbine outlet temperature (T_{Gout}) is equal to the work done for the adiabatic process occurring inside the combustion chamber. Where η_t is the turbine efficiency, P_{r0} is the compression ratio, and W is the compressor air flow rate.

$$T_{G_{out}} = T_{G_{in}}\left[1 - \left(1 - \frac{1}{(P_{ro}W)^{\frac{\gamma-1}{\gamma}}}\right)\eta_t\right] \quad (7)$$

3) Gas Turbine Transfer Function

The total output of the gas turbine (P_{GT}) is the sum of work done by the combustion gas in the turbine subtracted by the power used in the compressor. The transfer function of gas turbine output is as follows

$$P_{GT} = \frac{K_{GT}\{(T_{G,in} - T_{G,out}) - (T_{AC,out} - T_{AC,in})\}W_{AC,a}}{1 + T_{AC}s} \cdot \frac{K_{rec}(T_{cmb,out} - T_{AC,out})}{1 + T_{rec}}$$

(8)

4) Steam Turbine

The leftover high-pressure high-temperature exhaust gas from the gas turbine is utilized to heat water for the steam turbine through HRSG. The output power of the steam turbine (P_{ST}) and the transfer function is expressed in (5) where K_{ST} is the steam turbine power coefficient, T_e is the exhaust temperature, W_v is the steam flow rate, T_b is the boiler time constant and s is the Laplace coefficient.

$$P_{ST} = \frac{K_{ST} T_e W_v}{1 + T_b s} \quad (9)$$

C. PEMEC Modeling

The water electrolyzer implemented is PEMEC. The electrolyzer is based on [6].

1) PEMEC Electrical Model

The total electrical voltage (V_{cell}) of a single PEMEC cell equals the sum of open-circuit voltage (V_{OC}), activation overvoltage (V_{act}), and ohmic overvoltage (V_{ohm}). The equations for each parameter can be seen in the following equations:

$$V_{cell} = V_{OC} + V_{act} + V_{ohm} \quad (10)$$

$$V_{OC} = V_0 \frac{RT}{2F} ln\left(\frac{P_{H_2}\sqrt{P_{O_2}}}{a_{H_2O}}\right) \quad (11)$$

Where V_0 is open circuit voltage, R is gas constant, T is operating temperature, F is Faraday constant, and P_{H2}, P_{O2}, and a_{H2O} are the hydrogen, oxygen, and water pressure.

$$V_{act} = \frac{RT}{\alpha_{an} F} arcsinh\left(\frac{i}{2_{i,an}}\right) + \frac{RT}{\alpha_{cat} F} arcsinh\left(\frac{i}{2_{i,cat}}\right) \quad (12)$$

Where α_{an} and α_{cat} is the transfer coefficient of the anode and cathode, respectively. Symbol i represents current density and the subscript *an* and *cat* represents anode and cathode.

$$V_{ohm} = i \times \frac{\delta_m}{\sigma_m} \quad (13)$$

For the ohmic voltage, the resistance can be calculated by δm and σm, the cell membrane thickness, and conductivity.

2) PEMEC Thermal Model

The thermal model calculation of the PEMEC system is used for energy efficiency calculation (η_{en}). The energy efficiency can be calculated by (10) where n_{H2}, LHV and Q_e are the hydrogen molar flow rate, hydrogen lower heating value, and external power input.

$$\eta_{en} = \frac{n_{H_2} \times LHV}{Q_e} \quad (14)$$

D. Hydrogen Storage

The generated hydrogen is stored in a hydrogen tank. The tank pressure is the difference between the initial tank pressure (P_i) and the tank pressure (P_o). The value is obtained by the following equation [7]:

$$P_o - P_i = z\frac{n_{H_2} R T_o}{M_{H_2} V_T} \quad (15)$$

Where z is the pressure compressible factor. At room temperature with pressure below 2000 psi, it's equal to 1. n_{H2} is the molar flow rate of hydrogen entering the tank while M_{H2} is the hydrogen molar mass. R, T_o, and V_t are the ideal gas constant, tank operating temperature, and hydrogen tank volume.

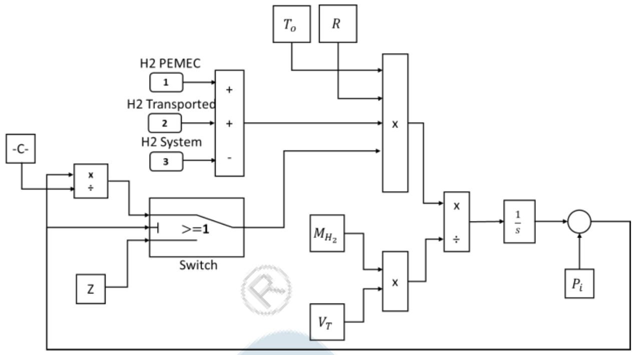

Figure 1. Hydrogen Tank Storage model in Simulink [8]

E. The capacity of the SOFC-TCC

The capacity of the SOFC-TCC generators is based on the equipment's thermal efficiency where it's determined by the ratio of net output (W_{net}) and the amount of heat supplied to the equipment (Q_s) [9].

IV. SIMULATION

A. Block Diagram of The Proposed System

The overall system block diagram is shown in Fig. 1. The system consists of one SOFC unit, one Gas/Steam Turbine combined cycle, one PEMEC electrolyzer, and one hydrogen storage unit.

The SOFC-TCC is interconnected with renewable energy wind and solar power in a core substation with an operating frequency of 50 Hz at 102 MW. The power demand detected will be satisfied by two power generators, the renewables and SOFC-TCC. Any surplus generated by renewable energy is allocated to hydrogen generation through PEMEC. Because renewable energy is fluctuating, there's bound to be unfulfilled power demand. The remaining power demand will be satisfied by the SOFC-TCC system. The SOFC, Gas Turbine and Steam Turbine's capacity was determined to be 0.46 p.u, 0.41 p.u, and 0.13 p.u.

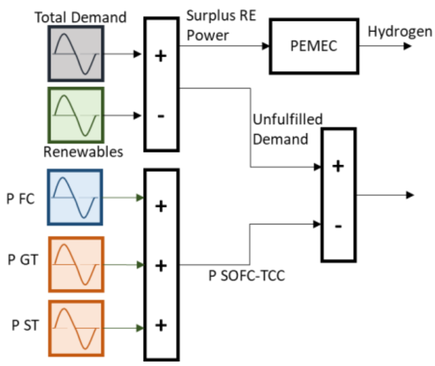

Figure 2. Simplified SOFC-TCC System Model

The hydrogen generated by PEMEC is stored in a hydrogen tank further to fuel the SOFC-TCC system. In case of insufficient hydrogen, the system also considers outsourcing hydrogen.

B. Block Diagram for SOFC-TCC System Control

Control of the system is mainly focused on the SOFC and Combined Cycle system. The SOFC is a fuel cell and therefore does not possess inertia potential. Hence, for it to satisfy load demand and respond appropriately to load changes, the SOFC is operated in governor-free control mode operation. The output of the cell is P_{FC} and exhaust heat. The heat is directed for utilization at the combined cycle gas turbine for compression and combustion. Control methods implemented are 'fuel flow control', 'exhaust air control', and 'exhaust air temperature control'.

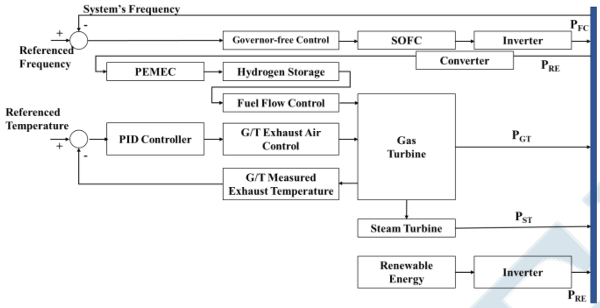

Figure 3. The complete SOFC-TCC block diagram

The block diagram of the fuel flow control and exhaust air control is mainly based on the combined cycle control method investigated in a previous study [10].

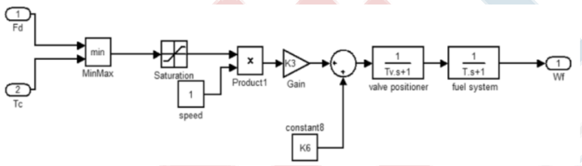

Figure 4. Governor Free-Control

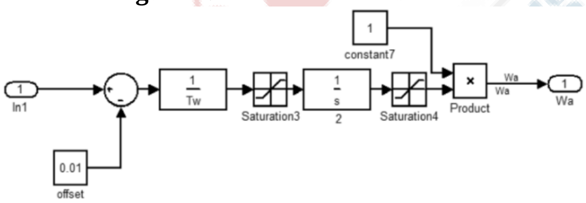

Figure 5. Exhaust Air Control

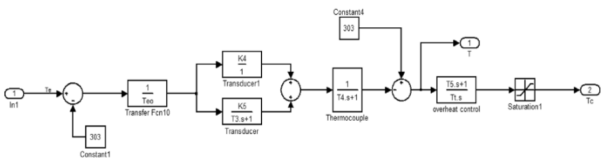

Figure 6. Exhaust Temperature Control

C. Frequency Deviation Control

Sudden changes in load demand cause frequency imbalance, therefore CCGT adjusts its output power according to load demand. The tolerable frequency deviation in this study is set to ±0.3 Hz.

The frequency deviation (Δw) of the turbine system can be expressed as [5]:

$$\Delta\omega = \frac{1}{Ms}\frac{1}{\omega_0}\Delta P \quad (16)$$

Where w_0 represents the grid frequency, M_s is the inertial constants of the turbine, and ΔP is the difference between demand (P_d) and generated power (P_{gen}).

$$\omega_0 = 1.0 + \omega \quad (17)$$

$$\Delta P = P_{gen} - P_d \quad (18)$$

V. RESULTS AND ANALYSIS

A. Power Demand and Renewable Power

The renewable power and the system's total demand are displayed in Fig.7 and Fig.8. After renewable power provides for the system's total demand, the surplus renewable power utilized for electrolysis and the remaining power demand can be seen in Fig.9 and Fig.10 respectively.

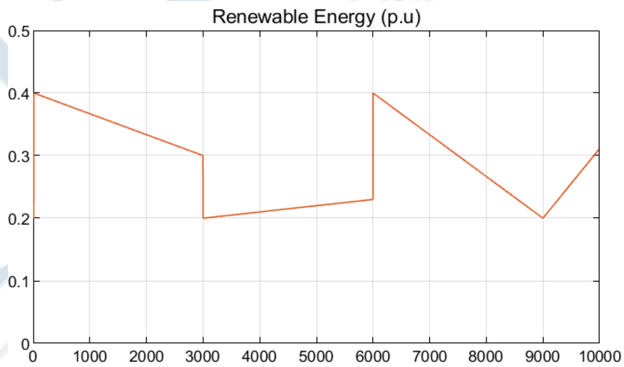

Figure 7. Renewable energy penetration to the system

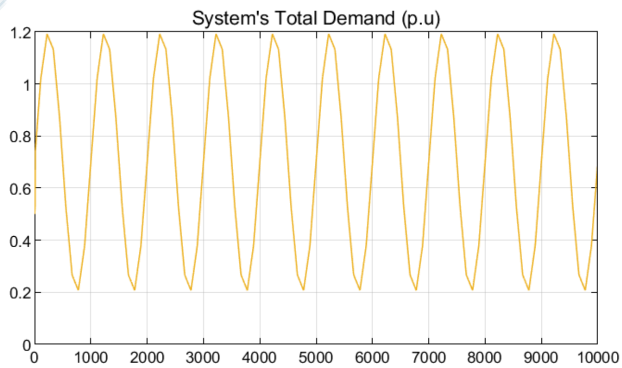

Figure 8. The system's total demand

ISSN (Online) 2456 -1304

International Journal of Science, Engineering and Management (IJSEM)

Volume 10 Issue 12 December 2023

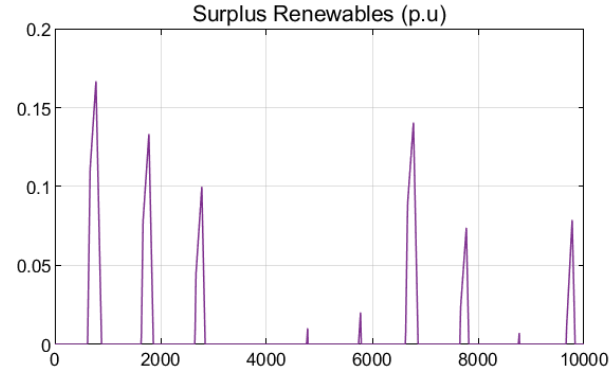

Figure 9. The surplus renewable power

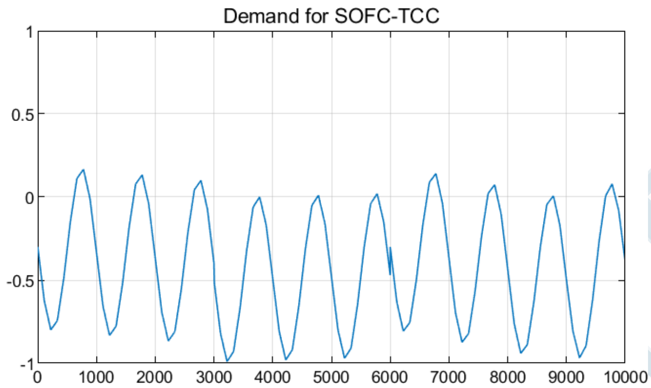

Figure 10. The unfulfilled power demand

B. SOFC-TCC System

The SOFC-TCC is required to provide for the remaining load demand while maintaining frequency deviation under the permissible margin. The total generated power is the summation of fuel cells, gas turbines, and steam turbines.

Figure 11 provides a detailed comparison between the power demand and the generated power. The difference between demanded and generated power can't be observed. Therefore, a side-by-side comparison is shown in Fig.12. Based on the figures, the SOFC-TCC system provides an immediate response to load demand, even in sudden variations in load demand.

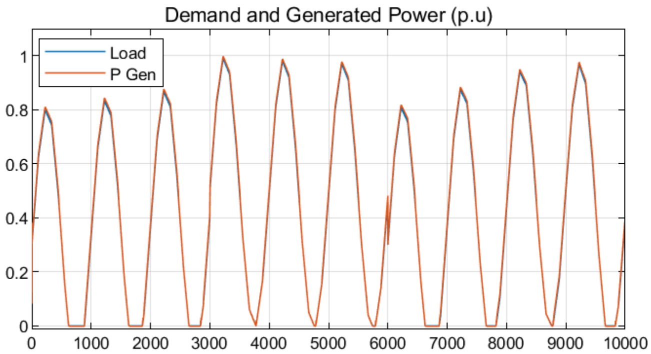

Figure 11. SOFC-TCC Demand and Power Generation

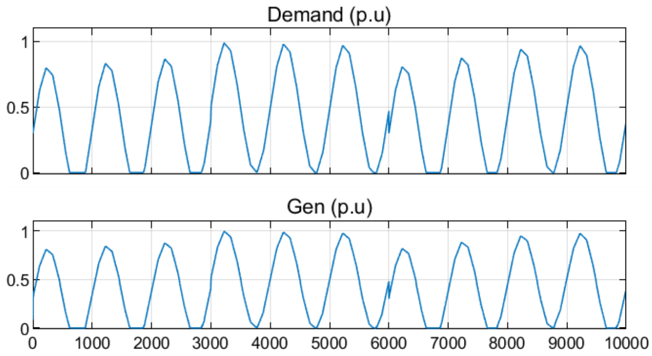

Figure 12. SOFC-TCC Demand and Power Generation Side by Side

The power generated by each component is shown in detail in the following figures. Observed that each component provides power according to the premeditated sizing.

As the SOFC is the first component, the SOFC takes care of the 'bottom' part of the power demand while the combined cycle provides for the remaining power.

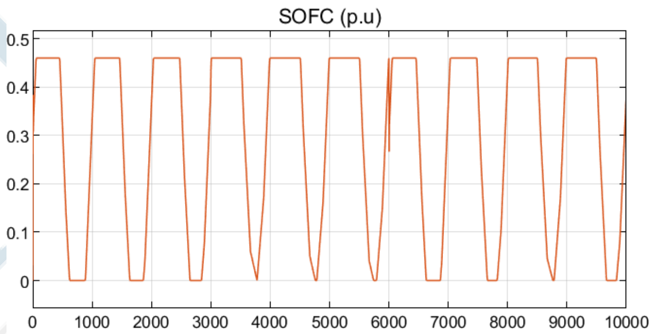

Figure 13. Power generated by SOFC

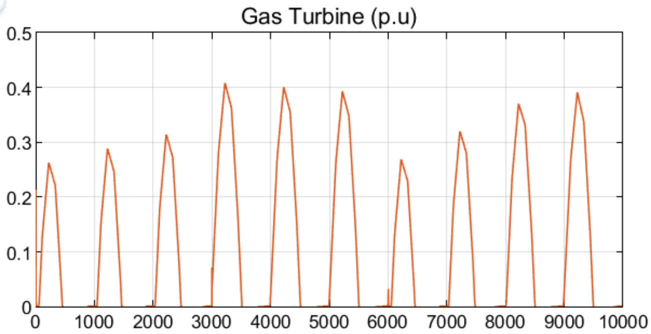

Figure 14. Power generated by Gas Turbine

IFERP connecting engineers... developing research

ISSN (Online) 2456 -1304

International Journal of Science, Engineering and Management (IJSEM)

Volume 10 Issue 12 December 2023

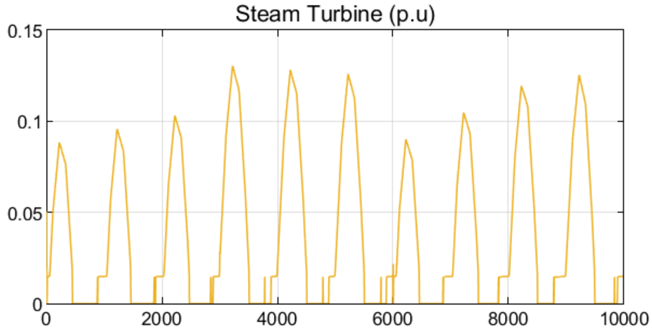

Figure 15. Power generated by steam turbine

C. Frequency Deviation

The system is set to operate on a frequency of 50 Hz with a tolerated deviation of ±0.3 Hz, which is equal to ±0.006 p.u in this study. The frequency deviation of the system is monitored throughout the cycle. At the beginning, an instant spike in frequency deviation is observed where it peaks at 0.006. Then when the system operates the frequency deviation ranges at ±0.005 p.u. The shown result is when the inertia constant is set to 15.

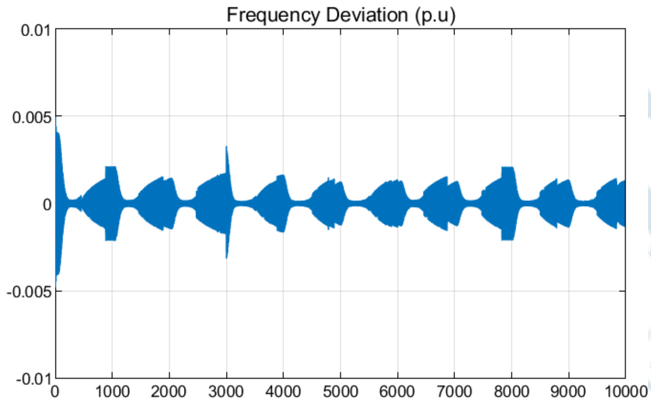

Figure 16. Frequency deviation of the system

D. Hydrogen Generation and Storage

The amount of hydrogen produced is determined by the previous equation shown in section III and heavily depends on the amount of surplus renewable power. Can be seen in Fig. 9 that the surplus renewable power throughout the cycle is inconsistent and available only for a short period in limited amounts.

With the surplus renewable power, the generated hydrogen is seen in Fig. 18 where the maximum of generated hydrogen is $15x10^{-4}$ mole, meanwhile, the required average hydrogen is $5x10^{4}$ and is shown in Fig. 17. Notice that the generated hydrogen is insufficient to provide for the whole SOFC-TCC system, therefore a hydrogen transport is also included. The amount of transported hydrogen is the difference between the required hydrogen and the available hydrogen in the tank and can be seen in Fig. 19.

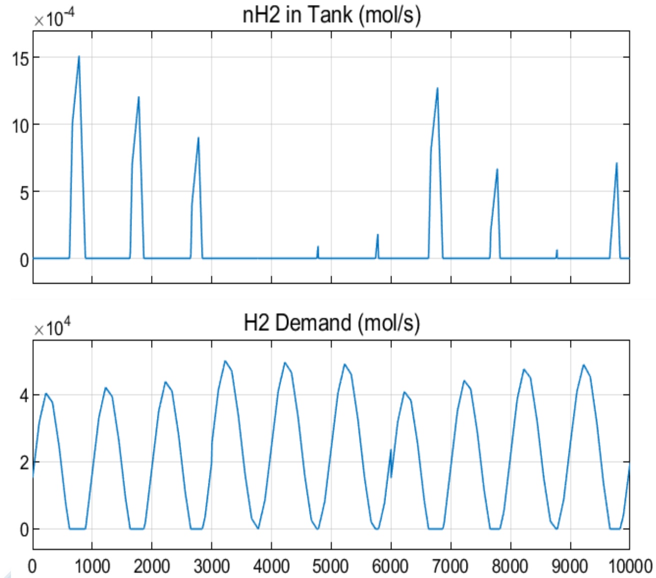

Figure 17. Hydrogen availability and hydrogen required by the system

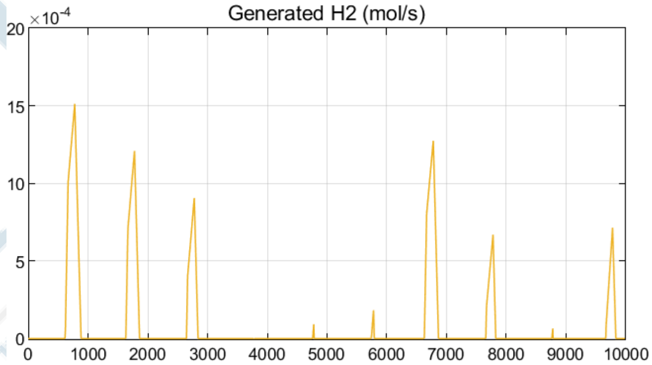

Figure 18. Hydrogen generated by PEMEC

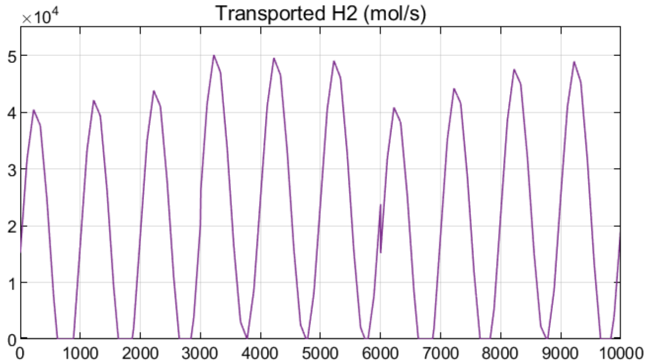

Figure 19. The additional amount of hydrogen transported

VI. CONCLUSION

The study for the dynamic design of a SOFC-TCC system with green hydrogen generation and storage has been performed. The system provides power for the residual power demand unfulfilled by renewable power.

Even with the highly fluctuating model of power demand, all the generator equipment shows robust response and managed to thoroughly provide power without any significant time delay. Which in return minimizes the occurrence of power difference between demand and supplied power.

For the combined cycle, as the first load following response and frequency deviation management highly depends on the inertial force, the inertia constant was determined as 15. This manages to keep the frequency deviation to be under permissible value thus keeping the system stable.

As the hydrogen generation relies solely on the available surplus renewable power, the generated hydrogen is limited and insufficient to provide for the whole system. This study suggests additional transported hydrogen to fulfill the system's needs. As the system shows a satisfactory response to the fluctuating power demand and manages to keep the frequency deviation under the threshold, the next target is to apply the system to actual renewable and power demand data.

REFERENCES

[1] S. Obara, "Dynamic-characteristics analysis of an independent microgrid consisting of a SOFC triple combined cycle power generation system and large-scale photovoltaics," Applied Energy, vol. 141, pp. 19–31, Mar. 2015, doi: 10.1016/j. apenergy. 2014.12.013.

[2] "Everitt and Veyo - Westinghouse Fuel Cell Combined Cycle Systems."

[3] Y. Kobayashi, Y. Ando, T. Kabata, M. Nishiura, K. Tomida, and N. Matake, "Extremely High-efficiency Thermal Power System-Solid Oxide Fuel Cell (SOFC) Triple Combined-cycle System," vol. 48, no. 3, 2011.

[4] R. P. O'Hayre, S.-W. Cha, W. G. Colella, and F. B. Prinz, Fuel cell fundamentals, Third edition. Hoboken, New Jersey: Wiley, 2016.

[5] H. Taniguchi, Power System Analysis Modeling and Simulation, Tokyo: Ohmsha, 2009, pp.64-65.

[6] N. Zheng, L. Duan, X. Wang, Z. Lu, and H. Zhang, "Thermodynamic performance analysis of a novel PEMEC-SOFC-based poly-generation system integrated mechanical compression and thermal energy storage," Energy Conversion and Management, vol. 265, p. 115770, Aug. 2022, doi: 10.1016/j.enconman. 2022.115770.

[7] H. Gorgun, "Dynamic modelling of a proton exchange membrane (PEM) electrolyzer," International Journal of Hydrogen Energy, vol. 31, no. 1, pp. 29–38, Jan. 2006, doi: 10.1016/j.ijhydene.2005.04.001.

[8] S. K. Bhuyan, P. K. Hota, and B. Panda, "Modeling, Control and Power Management Strategy of a Grid connected Hybrid Energy System," IJECE, vol. 8, no. 3, p. 1345, Jun. 2018, doi: 10.11591/ijece. v8i3.pp1345-1356.

[9] B. Tu et al., "Efficiency estimation of solid oxide fuel cell integrated with iso-octane pretreating system," Applied Thermal Engineering, vol. 236, p. 121298, 2024, doi: https://doi.org/10.1016/j.applthermaleng. 2023.121298.

[10] N. Hasan, J. N. Rai, and B. B. Arora, "Optimization of CCGT power plant and performance analysis using MATLAB/Simulink with actual operational data," SpringerPlus, vol. 3, no. 1, p. 275, Dec. 2014, doi: 10.1186/2193-1801-3-275.